Neutrino-induced Doppler-broadening study on oriented EuO single crystals

N. Stritt and J. Jolie
Institut de Physique, Université de Fribourg, Pérolles, CH-1700 Fribourg, Switzerland

M. Jentschel
Research Center Rossendorf, Dresden, Germany
and Institut Laue Langevin, Avenue des Martyrs 156X, F-38042 Grenoble Cedex, France

H. G. Börner and C. Doll
Institut Laue Langevin, Avenue des Martyrs 156X, F-38042 Grenoble Cedex, France

(Received 10 October 1997)

The motion of excited recoiling atoms produced by β decay of ^{152}Eu causes a Doppler broadening of subsequently emitted γ rays. The neutrino-induced Doppler-broadened γ-ray line shape is measured in oriented EuO single crystal targets using a high resolving power spectrometer. The motion and the slowing down of the emitting atoms depend on the forces exerted by the other atoms and on the direction of observation with respect to the crystal orientation. The comparison between measured and calculated γ-ray line shapes obtained by molecular dynamic simulation, permits to test different interatomic potentials and slowing down theories. The dependence of the observed line shape on the crystal orientation is also investigated.
[S0163-1829(98)01229-6]

I. INTRODUCTION

The two-axis flat-crystal GAMS4 spectrometer[1] installed at the Institut Laue Langevin allows the measurement of the Doppler broadening of γ rays caused by the motion of atoms in a solid state target. The recoil of the atoms is essentially induced by nuclear deexcitation after thermal neutron capture. The analysis of the small γ-ray broadening permits the determination of short lifetimes of nuclear excited states or the study of the slowing down process. The latter yields information on the form of the interatomic potential. The present study leads to information concerning the slowing down of atoms with kinetic energies of 1–3 eV in single crystals. In this work, the Doppler broadening of the measured γ rays originates from recoil induced by an electron capture. This reaction is a β decay process in which a nucleus captures an atomic electron. The nuclear reactions involved are

$$^{151}_{63}\mathrm{Eu}_{88}+n(25\ \mathrm{meV})\rightarrow{}^{152}_{63}\mathrm{Eu}_{89}+e^{-}\rightarrow{}^{152}_{62}\mathrm{Sm}_{90}+\nu. \quad (1)$$

The first reaction is a thermal neutron capture needed to make the unstable ^{152}Eu isotope that will partly decay by electron capture. In electron capture, a proton is transformed into a neutron and the resulting nucleus is identical to that which would be produced in a β^{+} decay. In order to conserve the leptonic charge during the β^{+} decay, the nucleus emits a neutrino. By this emission the atom acquires an impulse equivalent to the one the neutrino has when it leaves the nucleus. Since the neutrino has a well defined energy, a unique recoil velocity results. This is a particularity that normal β^{+} decay does not have because the simultaneous emission of a neutrino and a positron leads to a continuous range of initial recoil energies.

After the nuclear reaction, the atom starts to move a small distance away from its equilibrium lattice site. By pulling neighboring atoms away from their location it will slow down, stop, and start to move back to its initial position due to the forces exerted by the other atoms. As its energy decreases because of energy dissipation in the crystal by pulling more and more atoms away from their equilibrium position, the recoiling atom will return slowly to its equilibrium position and will finally thermalize. After the electron capture, the newly formed atomic nucleus can be created in an excited state. If the excited nucleus emits a γ ray during its motion, its energy will be Doppler shifted due to the velocity of the atom. The isotropic distribution of initial recoil directions leads then to the observation of a Doppler broadening of the line shape. The GAMS4 spectrometer, designed to measure γ-ray broadening in the order of $\Delta E/E=10^{-4}$ to 10^{-6}, detected the neutrino-induced Doppler (NID) broadening in solid state targets.[2] Because the velocity of the recoiling atoms depends on the forces and on the direction of motion, different structure should be observed in the Doppler-broadening γ-ray line shape for different potentials.

In the past couple of years, europium targets were analyzed in many forms and compositions.[2,3] However, the γ-ray line shapes were never measured using oriented single crystals targets in different orientations. Several techniques and theories were applied to calculate the possible line shape of the neutrino-induced Doppler broadening, such as the phonon creation model[2] and molecular dynamics (MD) simulations.[3] Here line shapes from neutrino-induced Doppler-broadening data obtained with EuO single crystals in different orientations are compared to the line shape calculated on the basis of MD simulations of the recoiling atoms. Recently we presented data from experiments performed in oriented single EuO crystals.[4] In the present paper those are combined with the results from another orientation

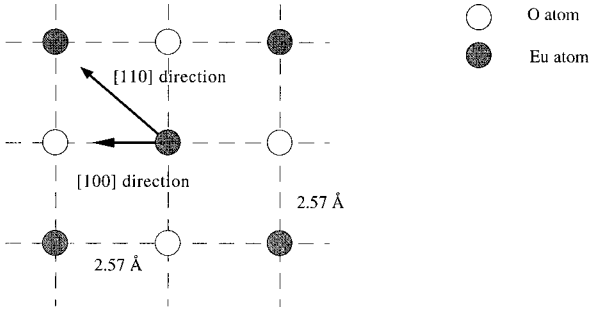

FIG. 1. Direction of observation toward the crystal spectrometer measured in a fcc EuO single crystal.

and a detailed account on the MD simulations used to analyze the data is given. To all measured data sets, different MD slowing down descriptions were applied. The different orientations were chosen to check the influence of the crystal structure on the γ-ray line shape. In a single crystal the ordering of the atoms is regular, and therefore, the anisotropy of the slowing down motion due to the direction of observation becomes relevant and is not smeared out as in polycrystalline structures. For instance in the [100] direction, the recoiling samarium atom will first encounter an oxygen atom while in the [110] direction the samarium atom will see an europium atom. Figure 1 shows the pattern seen by the recoiling atoms in the two different directions of observation analyzed in this work. In addition to the change in interatomic distance, as the potential is either attractive (Sm-O) or repulsive (Sm-Eu), the velocity of the recoiling atom and therefore the Doppler-broadened γ-ray line shape could vary with the direction of observation. All these effects give rise to the observation of different line shapes when the spectrometer is aligned along these two directions.

II. NEUTRINO-INDUCED DOPPLER BROADENING

The crucial Eu isotope in this experiment ^{151}Eu has a 47% natural abundance. The $\sim$9000 b neutron cross section of ^{151}Eu makes thermal neutron capture for this isotope preferential over the other natural isotope ^{153}Eu. After thermal neutron capture 36% of the formed ^{152}Eu atomic nuclei end up in the 0^- state at 45.6 keV. This isomeric state decays in 28% of the cases with a half-life of 9.3 h via electron capture forming ^{152}Sm. After electron capture a 1^- level at 963.4 keV in ^{152}Sm is populated (see Fig. 2). Some other states are also created in this process but they play a negligible role in this experiment, since electron capture represents 99.97% of the total feeding of the 963.4 keV level.[2] The 1^- level decays with a lifetime of 29(4) fs (Ref. 5) via emission of either a 963.4 keV γ ray to the ground state or a 841.6 keV γ ray to a long lived (τ=2.06 ns) 2^+ state. The last γ ray is followed by a 121.8 keV γ ray to the ground state. The recoil energy E_r given to the atom by the emission of a neutrino at the moment of the electron capture (β^+ decay) is given by

$$E_r=\frac{E_v^2}{2Mc^2}=\frac{Q^2}{2Mc^2}, \tag{2}$$

with Q the energy liberated in the reaction, M the atomic rest mass, c the velocity of light, and E_v the neutrino energy. Formula (2) gives a kinetic energy of $E_r\cong 3$ eV for the ^{152}Sm

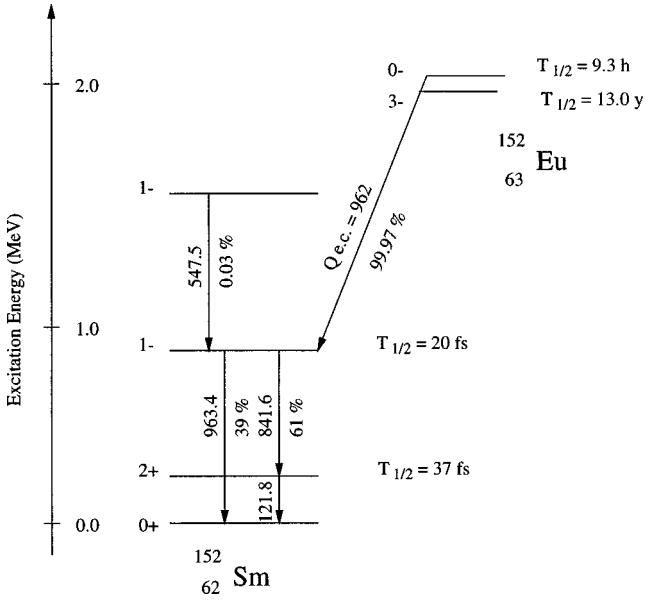

FIG. 2. The partial level scheme of ^{152}Eu and ^{152}Sm showing the nuclear reactions and transitions involved.

atom.[2] Therefore, the atom does not have sufficient energy to leave its lattice position in the crystal but will oscillate around its equilibrium position. However, the recoil energy is five times higher than the kinetic energy an Eu atom has due to thermal motion at the typical temperature inside a nuclear reactor.

III. SLOWING DOWN THEORIES AND MD SIMULATIONS

In order to analyze the data molecular dynamics codes were adapted for this particular experiment. The programs contain subroutines for the calculations of potentials and forces, and for the determination of time dependent positions and velocities for all atoms in the MD cells. Two programs were developed: one for thermalization of the EuO crystal to a given temperature and a second one which includes the extra recoil energy given by the neutrino emission to a samarium atom and then follows this atom during the appropriate time interval, which is in the order of a few hundreds of femtoseconds. The γ-ray line shape is calculated by simulating the motion of the atom using a constant energy and volume molecular dynamics method. The MD simulation programs solve numerically the Newtonian equations of motion for each atom using a Verlet algorithm.[6]

At the beginning of the simulation, the 1000 atoms of the MD cells are placed in a fcc array and periodic boundary conditions are applied in all three dimensions. No surface effects are considered in this approach and the crystal is seen as infinite. Before giving the initial kick simulating the recoil after neutrino emission ($v_r/c=6.54\times10^{-6}$) to the most central atom, all atoms in the MD cell are thermalized to the desired temperature by scaling the velocity of a few percent of the atoms chosen randomly in the MD cell each 20 fs. This is realized by a constant temperature algorithm[7] which brings the crystal slowly to the desired temperature without disturbing to much the system during the rescaling by leaving enough time for the relaxation of the atoms between each rescaling events. The process is simulated for a 15 ps period

TABLE I. Parameters of the different theoretical potentials for the EuO single crystal.

Potential	Eu-Eu	O-O	Eu-O
Born-Mayer	$A=42020$ eV	$A=2143.4$ eV	$A=10048.38$ eV
$V_1(r_{ij})$	$\rho=0.28508$ Å	$\rho=0.26396$ Å	$\rho=0.27449$ Å
Born-Mayer modified	$A=42020$ eV	$A=2143.4$ eV	$A=669.71$ eV
$V_2(r_{ij})$	$\rho=0.28508$ Å	$\rho=0.26396$ Å	$\rho=0.39536$ Å
Buckingham	$A=1715.0$ eV	$A=22764.3$ eV	$A=5045.4$ eV
$V_3(r_{ij})$	$\rho=0.317$ Å	$\rho=0.149$ Å	$\rho=0.290$ Å
	$C=0.0$ eV Å^6	$C=27.9$ eV Å^6	$C=34.0$ eV Å^6
Buckingham modified	$A=1715.0$ eV	$A=22764.3$ eV	$A=1148.9$ eV
$V_4(r_{ij})$	$\rho=0.317$ Å	$\rho=0.149$ Å	$\rho=0.3257$ Å
	$C=0.0$ eV Å^6	$C=27.9$ eV Å^6	$C=-140.1$ eV Å^6

with a time step of 0.5 fs. After 3 ps the cell has a constant temperature and the temperature algorithm is removed to allow the system to further relax. The velocity distribution of the equilibrated state of the atoms is described by a Maxwell-Boltzmann distribution.

Once thermalization is achieved, snapshots of positions and velocities of all 1000 atoms are recorded every 100 fs. This time interval insures that the thermal velocity direction of the atoms has significantly changed. The stored positions and velocities are then taken as initial conditions for the second MD program which starts by neutrino-emission-induced kick to the most central atom in the MD cell. As the neutrino energy is well defined, the neutrino-induced recoil is unique. The direction of motion is chosen in a random way by the MD program.

Another process affects the atomic recoil: after the reaction, an electron is missing, in most cases a K electron,[8] and the electron rearrangement process induces either an x-ray (in 90% of the cases) or an Auger electron emission (10%) (Ref. 9) by the refilling of the vacant orbit. Both processes impart also a small recoil to the atom. X rays and Auger electrons are emitted immediately after the electron capture decay, therefore at the beginning of the recoil. Since many electrons could leave the atom in the case of an Auger cascade it is possible to obtain a highly charge state for the recoiling atom. Therefore the interatomic potential will also be modified due to the Auger cascade. These extra recoils are small (5–15 %) compared to the neutrino-induced recoil, but are taken into account by the MD program for the most probable x-ray transitions and Auger emissions. In the simulations the recoil velocity of the K-LL, K-LM, K-MM, L-MM Auger transitions and the $K\alpha 1$, $K\alpha 2$, and $K\beta 1$ x-ray transitions were included. The MD program calculates using the Monte Carlo method the extra recoils and adds vectorially the additional recoil to the neutrino-induced recoil. The probabilities and energies of these transitions are taken from Ref. 10. The nucleus extra recoil velocity v_r is calculated for x ray emission by formula (3) and for Auger electron emission by formula (4):

$$\frac{v_r}{c}=\frac{E_\gamma}{Mc^2}, \tag{3}$$

$$\frac{v_r}{c}=\frac{\sqrt{E_e(E_e+1.022\ \text{MeV})}}{Mc^2}, \tag{4}$$

where M is the mass of the nucleus, c the velocity of light, E_γ the x-ray energy, and E_e the energy of the Auger electron. In Sec. V Auger cascades (loss of many successive Auger electrons), which could lead to a highly charged state for the atom, will be discussed in more detail.

Both MD programs can be easily changed to include different interatomic potentials. Because various descriptions and theories for interatomic potentials in solids exist,[11,12] several potentials were investigated and tested in this work by the crystal-NID method. Very few of these potentials were investigated before due to lack of experimental data in the energy range between 1–10 eV. Especially for this energy region the combination of the recent development of molecular dynamics simulations and the GAMS4 data yields opportunities to check interatomic potentials. Two potentials were analyzed in Ref. 4 and two others are developed in more details in this work. The four potentials used are only dependent on the distance (r_{ij}) between two atoms and are of the form:

$$V_k(r_{ij})=q_iq_j\frac{e^2}{4\pi\varepsilon_0}\frac{1}{r_{ij}}+A_{ij}\exp\left(-\frac{r_{ij}}{\rho_{ij}}\right)-\frac{C_{ij}}{r_{ij}^6}. \tag{5}$$

The parameters of the four different potentials are given in Table I. All potentials contain a Coulomb term for the ionic interaction due to the ionic nature of the EuO crystal bonding. To $V_1(r_{ij})$ only a Born-Mayer term $(C_{ij}=0)$ for the repulsive interaction is added, due to the overlap of the electron clouds.[13] As the Born-Mayer parameters are fitted to reproduce the Thomas-Fermi-Dirac calculation for identical atoms interaction, a sum rule theory was included to describe the interactions between different atoms.[14] $V_2(r_{ij})$ uses also the Born-Mayer potential form except that the Eu-O interaction parameters (A_{EuO}, ρ_{EuO}) were modified to reproduce the elastic constants, bulk modulus, as well as cohesion energy calculated by an accelerated convergence lattice summation based on Ewald procedures.[15] $V_3(r_{ij})$ takes into account a Buckingham dispersive term calculated using crystal parameters such as elastic constants, cohesion energy, and stable structure lattice constants.[3] $V_4(r_{ij})$ is similar to $V_3(r_{ij})$ but comes from another method of calculation with the same initial crystal parameters.[16,17] Compared to the initial potentials $V_1(r_{ij})$ and $V_3(r_{ij})$, respectively, the $V_2(r_{ij})$ and $V_4(r_{ij})$ potentials only differ by the interaction between Eu-O. For all potentials, q_i and q_j represent the ionic charges

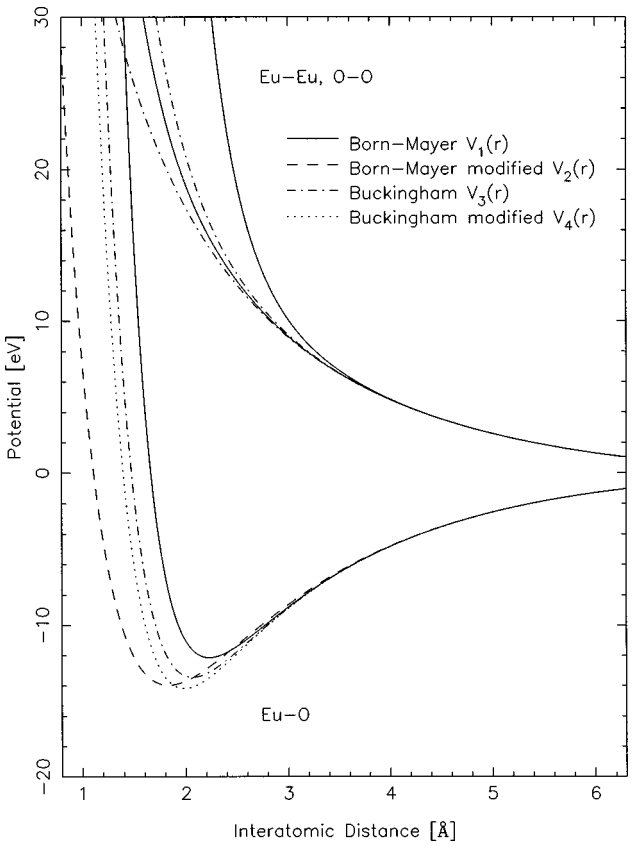

FIG. 3. Theoretical potentials for Eu-Eu, O-O, and Eu-O interactions. The two Born-Mayer and the two Buckingham-type potentials only differ by the Eu-O interaction (see text).

and are equal to $+2$ for Eu and Sm and -2 for O. The two Buckingham type potentials present an anomaly for short interatomic separation (<0.7 Å). At this short distance they become again attractive as the term $-C_{ij}/r_{ij}^6$ is dominant compared to the other two terms. In the present MD simulations this problem is negligible by the fact that the crystal atoms never come to that short distance because of their low kinetic energy.

The long-range Coulomb force is treated by a cutoff radius method forcing the force to go smoothly to zero at the cutoff distance. The cutoff radius was set for all potentials to 9.5 Å. Another method using an Ewald summation[18,19] instead of the cutoff radius method to treat the long-range force was tested in the MD simulations. The only potential investigated with this Ewald method is the Born-Mayer potential $[V_1(r_{ij})]$ due to the increase of CPU time. As already mentioned in Ref. 4, although after the reaction the recoiling atom is no longer a europium atom, no distinction is made for the calculation of the MD potential between Eu and Sm, the relative difference between the potential for Eu-Eu/Sm-Eu and Eu-O/Sm-O for $V_1(r_{ij})$ being less than 1.3%. Figure 3 shows the four different potentials used in the molecular dynamics simulations. The total potential energy seen by an Eu atom for two potentials is illustrated in Fig. 4. These two figures demonstrate that the Eu atom needs more kinetic energy (or a higher initial recoil) if it wants to travel the same distance under the Born-Mayer potential than under the Buckingham. Once the atom has reached a certain velocity, the slowing down process is thus much faster for the Born-Mayer simulations and therefore thermalization of the recoiling atom is achieved more rapidly. The modified Born-Mayer potential $V_2(r_{ij})$ is the least repulsive potential for the Eu-O interaction at short distance.

The second simulation program records, after the kick given to the central atom by the neutrino emission, the motion and velocities of the recoiling atom during 125 fs. This time interval corresponds to four times the expected 963.4 keV nuclear state lifetime. As the probability of the γ-ray emission is given by

$$P_\gamma(t) \propto \exp\left(\frac{-t}{\tau}\right), \tag{6}$$

where τ is the lifetime of the excited nuclear state, the contribution of longer times to the Doppler-broadened line shape can be neglected since the number of γ rays emitted after 4τ is less than 2%. The measurement of many recoils events and many Doppler-shifted γ rays will result in a blue-red-

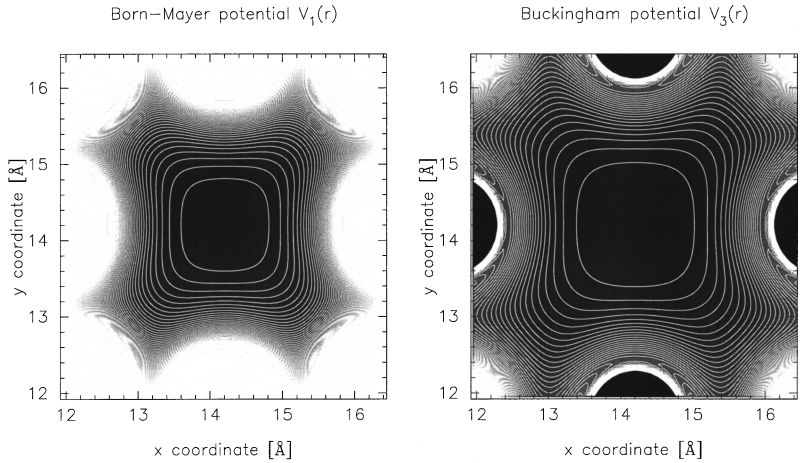

FIG. 4. The total interatomic potential for the Born-Mayer (left) and for the Buckingham (right) potential. The full lines represent the equipotential surface. The difference between two equipotential lines represents 6.0 eV and the maximum potential value is cut at 300 eV. The (x,y) positions of the Eu atoms are (11.58,11.58), (11.58,16.73), (16.73,11.58), (16.73,16.73) and the positions of the O atoms are (11.58,14.16), (14.16,11.58), (14.16,16.73), (16.73,14.16).

broadened γ-ray line shape. The neutrino-induced Doppler-broadened γ-ray line shape, obtained by the motion of the atoms in the bulk material, is described by the formula[20]

$$I(E)=c\sum_i \int_0^\infty e^{-t/\tau}\delta\left[E-E_\gamma\left(1+\frac{\mathbf{v}_i(t)\cdot\mathbf{n}}{c}\right)\right]dt, \quad (7)$$

with C a constant used for normalization, τ the excited nuclear state lifetime, E_γ the nonshifted energy of the transition, $\mathbf{v}_i(t)$ the velocity vector of the ith simulated atom at the moment of emission as calculated by the MD programs, $\mathbf{n}$ the relative direction of observation and c the velocity of light. The index (i) ranges generally from 1–1500 and represents the number of recoil events calculated by the molecular dynamics simulations. The natural linewidth of the line ($\Gamma_{963\ \mathrm{keV}}\cong\hbar/\tau_{963\ \mathrm{keV}}=0.0235$ eV) is neglected in the calculation of the line shape since its effect contributes to less than 1% of the total broadening ($\cong 10$ eV). The symmetries of the EuO crystalline structure are also employed to increase statistics for the calculation of the line shape. For example a simulated recoil in the [100] direction is identical to a simulated recoil in the [010] direction, however, the contribution to the line shape will be different. Using thus these symmetries, one can construct a γ-ray Doppler-broadened line shape with less recoils events.

Once the motion and velocity $[\mathbf{v}_i(t)]$ of the recoiling atoms are stored, and once the instrumental response is measured, the γ-ray line shape can be evaluated for different lifetime values (τ) from the MD slowing down simulations. Such line shapes are then fitted to the measured data using the least square fitting routine GRIDDLE,[21] with the lifetime and experimentally related numbers (background, intensity, etc.) as free parameters. As a result of this procedure a lifetime value τ and a χ^2 per degree of freedom are obtained. Both values permit to quantify the agreement/disagreement between theory (MD simulation of the slowing down) and the experiment (NID data). A typical MD simulation CPU time for the following of one recoil event during 125 fs is equal to 250 sec on a HP 9000 Model 712/80 computer.

IV. NEUTRINO-INDUCED DOPPLER-BROADENING MEASUREMENT

A. Target preparation

The data were measured using fcc single crystals of EuO. These magenta crystals have a lattice constant of 5.141 Å and a NaCl crystalline structure.[22] The high melting temperature [2289(8) K (Ref. 23)] insures that the fcc crystalline structure of the EuO crystal stays stable during the neutron irradiation inside the nuclear reactor. These crystals have a density of 8.20 g/cm^3 and were grown by a high-temperature chemical transport method[24] for the first experiment and by a solution sintering process[25] for the second one.

Two orientations, the [100] and the [110], were investigated in this experiment. The first orientation comprises seven pieces of EuO single crystal embedded in a two parts graphite matrix. The total mass of the EuO crystals was equal to 672 mg. They were placed in the matrix with the [100] orientation in the direction of the spectrometer. Each target (closed matrix containing the EuO crystals) is then inserted in a graphite holder with dimensions of

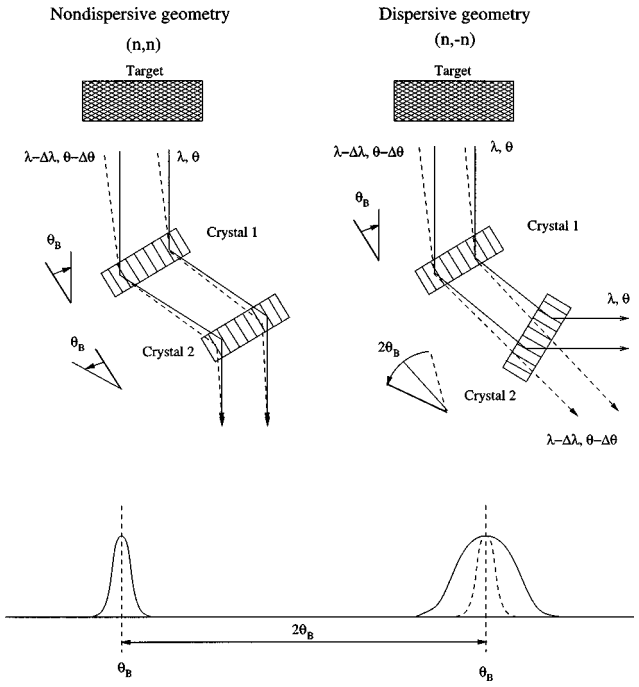

FIG. 5. Schematic representation of the two modes that can be obtained with two successive crystals. The full line corresponds to γ rays with a wavelength λ, the dashed to those with a wavelength $\lambda-\Delta\lambda$.

25 mm×18 mm×2 mm in order to be placed safely inside the reactor. Three graphite holders were necessary to contain the different matrix and were placed parallel one after the other with the 25 mm×2 mm oriented surface looking in the direction of the spectrometer. As the natural isotope ^{151}Eu has a high neutron cross section, small crystals (mm size) are sufficient to have enough intensity for this kind of measurements. For the second orientation, the same technique and preparation were used. Again three targets holder were needed to place the different single crystals for a total mass of EuO of 767.8 mg. The orientations of all crystals for both directions were checked with back-reflection Laue picture created by x-ray irradiation.[26] The sets of oriented EuO targets were placed at the GAMS4 in-pile target position of the Institut Laue Langevin, where they are irradiated with a neutron flux of 5×10^{14} cm^{-2} s^{-1}.

B. The GAMS4 spectrometer

The instrument used in the present work is a two-axis flat-crystal spectrometer. It is composed of two flat hyperpure Si crystals, several collimators and moving tables that permit to rock the two crystals. The γ-ray detection is then done with a semiconductor Germanium detector. A complete description of the mechanism and operating system as well as of the extraction of the data can be found in Ref. 1. The spectrometer can operate under two modes: the nondispersive and dispersive modes. The nondispersive mode allows one, as the two crystals are parallel (see Fig. 5), to measure the instrumental response of the line by setting the first crystal to the position to have the Bragg reflection (θ_B) for a given energy and by rocking the second one around this

TABLE II. Fitted values of the excess width in fringes ($1F = 0.04$ arcsec) (Ref. 1) for the transitions from long lived states obtained with the two orientations.

Transition energy [keV]	Orientation $[xyz]$	Order (n,m)	No. of scans	χ^2 per degree of freedom	Fitted excess width $[F]$	Error [%]
121.8	[100]	(1,1)	10	1.0937	0.308(27)	8.76
221.2	[100]	(2,2)	13	0.9750	0.246(69)	27.64
221.2	[110]	(2,2)	11	1.0615	0.216(63)	29.16

angle. In this case the only broadening the spectrometer measures is due to the instrumental response of both crystals when they are irradiated by γ rays of a certain energy range. The response of the spectrometer is described by dynamical diffraction theory folded with a small Gaussian extra broadening (excess width).[27] The second mode (dispersive mode) uses for the second crystal the mirror image angle. In that case the second crystal is again rocked but around this mirror image with respect to the direction of the diffracted beam$(-\theta_B)$ (see Fig. 5). With this method an extra broadening which is not related to the instrumental response but to physical processes such as Doppler broadening and the natural linewidth can be measured. In dispersive scans, the total line shape is described by three contributions: (i) the instrumental response, (ii) Doppler broadening due to the thermal motion of the atoms, and (iii) by recoil-induced Doppler broadening. All these contributions are analyzed separately. With these two modes of operation, a γ-ray peak can be fully described. Once the instrumental response is known from nondispersive scans for a given transition, one can measure the extra broadening caused by the motion of the atom emitting this γ ray. The GAMS4 spectrometer can also run using different orders of reflection. The higher the order becomes the more information one can obtain from a line. Intensity and statistical problems limit the use of too high orders as diffraction theory predicts in most cases a smaller intensity with increasing order of reflection.[1]

During the two sets of measurements, different γ-ray transitions were analyzed. The principal lines of interest for this nucleus are the 841.6 and 963.4 keV transitions to measure the broadening due to the motion of the emitting ^{152}Sm atom. The 121.8 and 221.2 keV transitions are needed to measure the extra broadening due to thermal motion of the atom. Since the 1^- state at 963.4 keV reached after electron capture is short lived, the Doppler broadening of the 841.6 and 963.4 keV transitions comes essentially from the recoil and the slowing down after the neutrino emission. In contrast the 121.8 and 221 keV transitions are created by decay of long lived states with lifetimes in the ns time interval.[28] In these last cases, the emitting atom has sufficient time to slow down and to thermalize. Therefore, the extra broadening in the γ-ray line shape is caused essentially by the thermal motion.

C. Measurement of the broadening due to thermal motion

The thermal broadening was determined using the 121.8 keV transition from the 2^+ state and the 221.2 keV transition (a prompt γ ray emitted after neutron capture). To be able to determine the extra thermal broadening coming from transitions emitted from long lived nuclear states, the spectrometer response function has to be known. The spectrometer response can be directly measured in nondispersive mode with both spectrometer crystals parallel. The results of these nondispersive scans in the different orientations are given in Table II. Although the error on the fitted excess width is relatively high in some cases (29.2%), the effect on the fitted thermal velocity obtained from dispersive scans of the same transition is not significant (less than 5% in the worst case).

A comparison between the line shape obtained in the [100] and the [110] orientation can be seen for the 221.2 keV transition in Fig. 6. The fitted thermal velocities and the corresponding crystal temperatures obtained with the least square fit of the data given by the program GRIDDLE are shown in Table III. The adopted value for the thermal velocity, taken as the weighted average from the two different lines and from the two orientations, is equal to 537(24) m/s. The corresponding crystal temperature calculated by the Maxwell-Boltzmann theory with the measured thermal velocity is equal to 1759(154) K. This temperature is close to

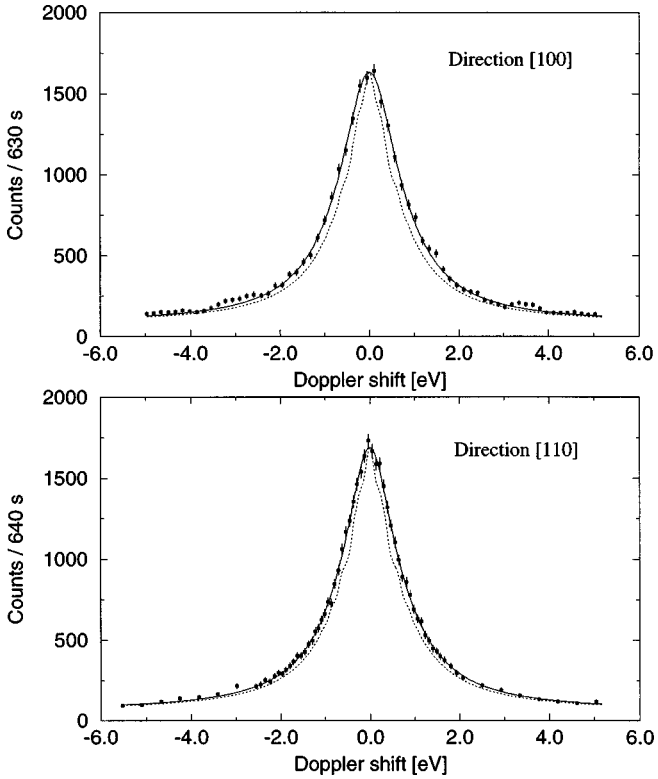

FIG. 6. The γ-ray line shape of the 221.2 keV transition in first order of reflection. The dotted line represents the instrumental response (diffraction theory curve folded with a small Gaussian) and the full line is the fit which includes the thermal broadening. The upper part shows the sum of 21 scans in the [100] orientation and the lower part the sum of 16 scans in the [110] orientation.

TABLE III. Fitted values of the thermal velocity for the transition from long lived states obtained with the two orientations.

Transition energy [keV]	Orientation [xyz]	Order (n,m)	No. of scans	Lifetime used [ns]	χ^2 per degree of freedom	Thermal velocity [m/s]	Crystal temperature [K]
121.8	[100]	(1,−1)	12	2.06	1.1096	625 (53)	2379 (403)
221.2	[100]	(2,−2)	21	200.0	1.1328	570 (37)	1979 (257)
221.2	[110]	(2,−2)	16	200.0	1.0186	428 (36)	1116 (188)

the calculated temperature of ~1600 K for an EuO crystal with the specific irradiation conditions at the target position inside the ILL nuclear reactor. The discrepancies between the different measurements and orientations are probably related to statistical problems. In several other experiments,[4,29] there are still differences between two sets of identical measurements about the effective targets temperature. The correctness of the experimental temperature determination using the depopulation of long living states is yet not evident and can be influenced by instrumental procedures and analysis. Further investigations will follow to solve these target temperature problems.

As discrepancies exist and because the measured temperature varies from 2379 to 1116 K (see Table III), MD simulations were started with different crystal temperatures to see the influence on the fitted nuclear lifetime of the 841.6 keV line. This was realized by starting the molecular dynamics simulations with different crystal temperatures. Figure 7 shows the Maxwell-Boltzmann distribution of the Eu atoms in the cell for three different temperatures calculated by the MD program using a Buckingham-type potential. Simulations at 700 and 2170 K for two potentials were done and the influence on the 963.4 keV nuclear state lifetime is shown in Table IV. The values differ by less than 5% between simulation done at 700 and 2170 K except for the Buckingham potential in the [110] orientation where the difference equals 13.7%. While the influence on the positions and thermal motions of the atoms in the crystal is great, a minor effect on the nuclear lifetime measurement is found. In the following MD calculations the average temperature of 2170 K calculated from the 121.8 and 221.2 keV transitions in the [100] orientation was adopted.[4]

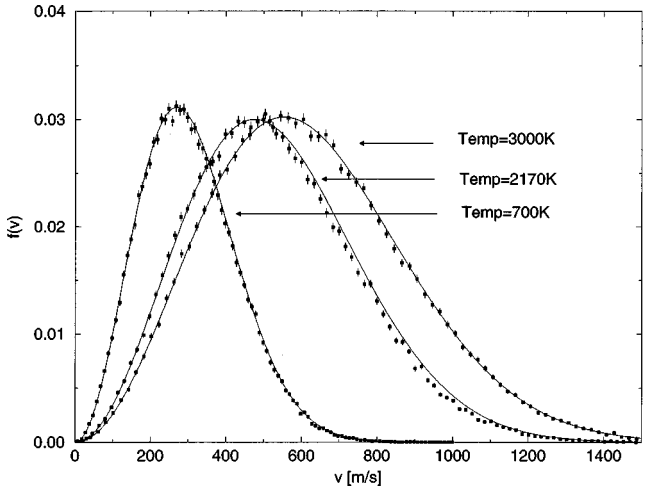

FIG. 7. Distribution of the thermal velocity of 250×500 Eu atoms in a EuO lattice at different temperature. The points represent the molecular dynamics simulations and the full line the Maxwell-Boltzmann distribution theoretical curve for the mentioned temperature.

D. Measurement of the neutrino-induced Doppler broadening

The 841.6 keV transition was chosen to investigate the influence of the potential on the 963.4 keV nuclear state lifetime and to check the change in the line shape due to crystal orientations. This transition has several advantages. On one hand the nuclear lifetime is known by another method[5] which permits us to select which potential is suitable for the interaction in the crystal. As the lifetime value is known, the interatomic potential must be chosen to reproduce this lifetime. If a wrong slowing down theory is chosen, a wrong lifetime value will be obtained. On the other hand the lifetime is in the right order of magnitude (~30 fs) to be analyzed by the NID method and to be simulated by the MD programs with reasonable CPU time. This transition also has sufficient intensity to be measured with the high resolving power crystal spectrometer.

The instrumental response function for this transition was measured in both directions. The fitted excess width measured with nondispersive scans in third order of reflection for the 841.6 keV transition is equal to 0.1864 ± 0.0075 fringes for the [100] orientation and is equal to 0.20765 ± 0.0077 fringes for the [110] orientation (see Fig. 8). One fringe corresponds to an angle of 0.04 arcsec. For the 841.6 keV transition, the motion of the emitting atom due to neutrino emission and then the slowing down due to the interatomic potential are responsible for the Doppler broadening of the line shape measured in the dispersive geometry. Figure 8 shows the third order of reflection measured line shape of the 841.6 keV transition for the [110] orientation. The difference in line shape for the 841.6 keV transition in the [100] and [110] orientations is illustrated in Fig. 9 using the MD Buckingham potential V_3. This figure shows that the slowing down of the recoiling atom is slightly dependent on the direction of observation. Although the recoil energy is small compared to usual crystal-GRID measurements,[30] a contrast between the two directions of observation is still measurable and shows that the difference is statistically significant. As the lifetime fitted with the simulation using the Buckingham-type potential differs by a few fs for the two orientations (see Table V), a forced fit to the [110] measured data was also realized with the lifetime of the [100] orientation taken as a fixed parameter. This shows that the difference is essentially due to the direction of observation and not due to the differ-

TABLE IV. Influence of the crystal temperature on the lifetime of the 963.4 keV nuclear state.

Potential	Orientation [xyz]	No. MD recoils	MD crystal temperature [K]	χ^2 per degree of freedom	Fitted lifetime [fs]
Born-Mayer $V_1(r_{ij})$	[100]	1500	700	1.1530	18.6(0.8)[a]
	[100]	1500	2170	1.1493	17.2(0.8)
	[110]	1500	700	1.1448	19.8(0.9)
	[110]	1500	2170	1.1484	20.8(1.2)
Buckingham $V_3(r_{ij})$	[100]	1500	700	1.1553	26.7(1.1)
	[100]	1500	2170	1.1487	26.9(1.2)
	[110]	1500	700	1.1439	27.2(1.3)
	[110]	1500	2170	1.1495	31.5(1.7)

[a]The molecular dynamics simulations were realized without the x-ray and Auger emission subroutine.

ence in the lifetime value. The [100] orientation shows a more broadened line shape mainly due to the smaller separation and the attractive form of the potential the Eu recoiling atom sees moving in this particular direction (see Figs. 1 and 3). Although the γ-ray line shape measured in one direction is calculated from initial recoils in all directions, the greatest Doppler shifts arise when the atoms are moving in the direction of the spectrometer.

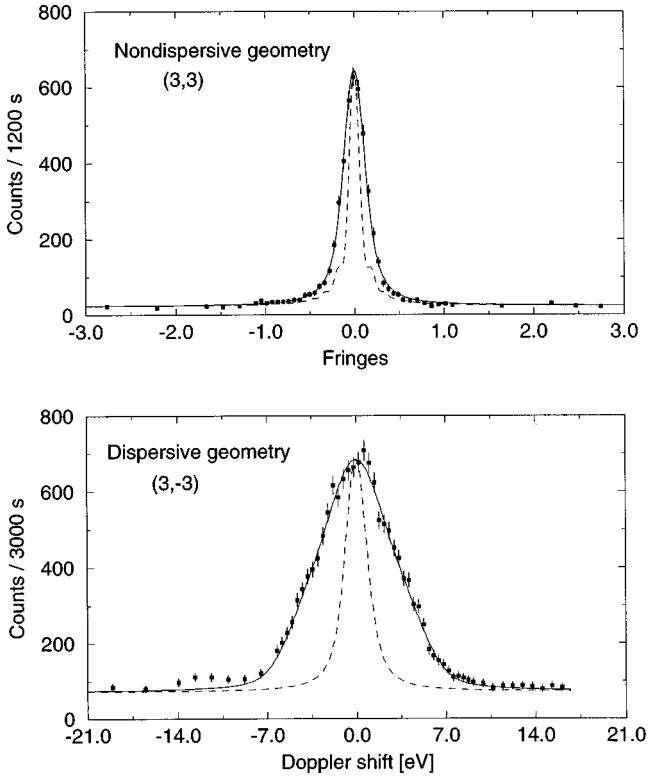

FIG. 8. The γ-ray line shape of the 841.6 keV transition in third order of reflection obtained from a sum of 10 nondispersive scans (top) and from a sum of 25 dispersive scans (bottom) for the [110] orientation. In the upper part the dotted line represents the diffraction theory curve and the full line stands for the diffraction curve folded with a Gaussian given by the mentioned fitted excess width. In the lower part, the dotted line corresponds to the instrumental response as determined in the upper part and the full line is the fit representing a lifetime of 31.2(1.6) fs. The two figures have the same angular range. The Buckingham potential is used in the simulations for the calculation of the lifetime.

V. DATA ANALYSIS AND RESULTS

The five different MD potentials discussed in Sec. III were used to analyze the measured line shapes. Table V lists the results of the fitted 963.4 keV nuclear state lifetime. All the Born-Mayer potentials give a lifetime value smaller than the one mentioned in the literature.[5] This reflects the fact that the Born-Mayer V_1, V_2, and V_5 potentials are too repulsive at short distances. Even with a low recoil energy, where the atom does not move far from its lattice position, the repul-

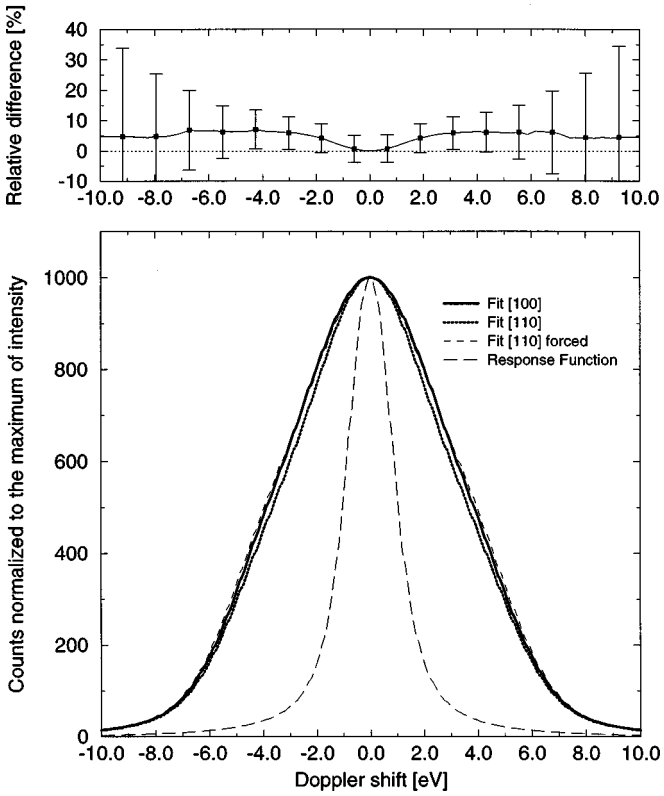

FIG. 9. The γ-ray line shape of the 841.6 keV transition in third order of reflection. The full line represents the [100] orientation fit and the dotted line the [110] orientation fit. The dashed line represents a forced fit to the data using the lifetime of the [100] orientation instead of leaving the lifetime as free parameter (see text). Also shown is the instrumental response of the spectrometer. The upper part of the figure shows the relative difference $(I_{[100]} - I_{[110]}/I_{[100]})$ between the two orientations.

TABLE V. Fitted lifetime for the two orientations and the five different MD theoretical potentials. The temperature of the crystal is set for all MD simulations to 2170 K.

Potential	No. MD recoils	Orientation [xyz]	χ^2 per degree of freedom	Fitted lifetime [fs]
Born-Mayer $V_1(r_{ij})$	1500	[100]	1.1493	17.2(0.8)
	1500	[110]	1.1484	20.8(1.2)
		[100] and [110]		19.0(0.7)[a]
Born-Mayer modified $V_2(r_{ij})$	1500	[100]	1.1486	25.2(1.1)
	1500	[110]	1.1496	27.0(1.4)
		[100] and [110]		26.1(0.9)[a]
Buckingham $V_3(r_{ij})$	3000	[100]	1.1486	26.1(1.2)
	3000	[110]	1.1482	31.2(1.6)
		[100] and [110]		28.7(1.0)[a]
Buckingham modified $V_4(r_{ij})$	3000	[100]	1.1489	29.2(1.3)
	3000	[110]	1.1506	37.6(2.1)
		[100] and [110]		33.4(1.2)[a]
Born-Mayer+Ewald $V_5(r_{ij})$	1500	[100]	1.1513	21.2(0.9)
	1500	[110]	1.1450	25.2(1.1)
		[100] and [110]		23.2(0.7)[a]

[a]Average lifetime taken from the [100] and the [110] orientation.

sive Born-Mayer potential (see Fig. 4) is strongly felt. This results in a lowering of the measured lifetime as the atom has less freedom to move around its lattice position and therefore the lifetime fitted decreases so to have the same Doppler shift. The modified Born-Mayer potential V_2 gives, however, a much better result. Although its parameters correspond to the least repulsive interatomic potential for the Eu-O at small distance, the Eu-Eu and O-O interactions is less adequate to reproduce the lifetime as the slowing down takes place more rapidly due to the repulsive part. For the Buckingham potential V_3 the lifetime fitted 28.7(1.0) fs is in very good agreement with the literature value of 29(4) fs and also gives the smallest χ^2 per degree of freedom for both directions (except for the [110] fit with V_5). The Buckingham modified potential V_4 shows some problems especially in the [110] direction which is probably caused by the form of the Eu-O interaction around the equilibrium position (see Fig. 3). The repulsive part of this interaction is too weak between 1–2 Å and increases the lifetime of the nuclear state under study. Although the difference between the two potentials is not very large, the result on the lifetime is quite pronounced (especially in the [110] direction). The result of the Ewald method using the Born-Mayer potential V_5 is relatively close to the cutoff radius method V_1 (see Table V). As no significant changes are observed with this method when an appropriate long cutoff radius is chosen, it is worthless due to CPU time consumption in the EuO case to perform this kind of MD simulations.

In the second MD program, the neutrino-induced recoil direction as well as the energy and direction of the x-ray- or Auger-emission-induced recoil are chosen randomly by a set of selected random numbers. The influence of the random numbers and statistical errors on a fitted lifetime is shown in Table VI for a given potential in both directions [100] and [110]. As can be seen in this table the relative difference between the lifetime obtained with both sets of random numbers and the mean lifetime value (see last two row of Table VI) never exceeds 8% for a given orientation, when enough events (1500 recoils) are considered.

Another influence on the determined nuclear lifetime

TABLE VI. Influence of the random number generator on the deduced lifetime of the 963.4 keV nuclear state in ^{152}Sm. The Buckingham-type potential $V_3(r_{ij})$ is used. The measured 841.6 keV line shape was fitted.

Random set	No. MD recoils	Orientation [xyz]	χ^2 per degree of freedom	Fitted lifetime [fs]	Error [%]
1	1500	[100]	1.1486	27.8 (1.3)	4.67
	1500	[110]	1.1495	31.5 (1.8)	5.71
2	1500	[100]	1.1486	24.5 (1.1)	4.49
	1500	[110]	1.1475	31.1 (1.6)	5.15
3	1500	[100]	1.1487	28.0 (1.2)	4.29
	1500	[110]	1.1481	33.2 (1.8)	5.42
4	1500	[100]	1.1491	24.8 (1.1)	4.44
	1500	[110]	1.1480	30.0 (1.6)	5.33
All sets 1–4	6000	[100]	1.1486	26.3 (1.2)	4.56
	6000	[110]	1.1481	31.4 (1.7)	5.41

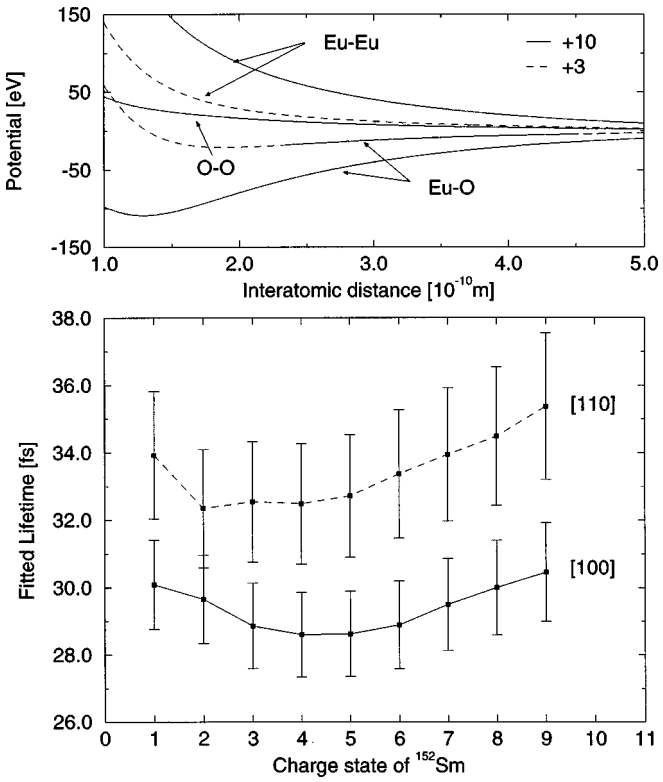

FIG. 10. Dependence of the fitted lifetime of the 963.4 keV nuclear level in ^{152}Sm on the charge state of the recoiling ion in the EuO single crystal. The Buckingham-type potential $V_3(r_{ij})$ is used during the simulations. The number of recoiling events is equal to 250. The result is a fit to a sum of 28 scans for the [100] orientation and a sum of 25 scans for the [110] orientation. The upper part shows the interatomic potential for two different charge states. A charge state of $+1$ has no physical meaning, but was also simulated for comparison.

value is the charge state of the recoiling atom. All the precedent MD simulations were realized with a charge state of $+2$ for the recoiling Sm atom. This $+2$ charge state follows from the β decay, because of charge conservation during the nuclear reaction. The charge state of the Sm atom could increase in the case of Auger cascades and can range from $+2$ to $+10$.[31] In the simulation the charge state does have a great effect on the local environment especially for high charge states. The crystalline structure can be destroyed around the recoiling atom by the Coulomb interaction. As the charge state of the Sm atom takes a high value, the attractive interaction between the Sm-O atoms as well as the repulsive potential between Sm-Eu changes significantly (in our case the Buckingham potential see the upper part of Fig. 10). The four nearest neighbors, the O atoms, approach in the first 10–20 fs interval extremely close to the Sm atom, the so-called Coulomb implosion of the crystal. Then the repulsive potential between the four O atoms overcomes the attractive part of the Sm-O potential and the O atoms move away from the Sm atom. During this process of implosion and afterwards explosion, the O atoms gain an enormous kinetic energy which can in the case of high charge state destroy the crystalline structure of the cell. This kind of process does not play any role for $+2$ charge state because in this case the distance between neighbor atoms never becomes so small that the atoms gain enough energy to destroy the entire MD cell. In any cases, as the probability to have an emission of an Auger electron to fill the K hole is relatively low (10%) for the Sm atom, the influence of the charge state on the fitted nuclear lifetime is not pronounced.

Some MD simulations were made as follows to investigate the influence of the charge state. When an Auger emission occurs the charge state of the recoiling Sm atom is changed to the desired value ($+2$ to $+10$) assuming an Auger cascade and keeping at the same time all the other potential parameters identical. Figure 10 shows the influence of the charge state in the simulations and reveals the minor role played by the charge state, because of the low probability of Auger emission. The increase of the nuclear lifetime for higher charge states is related to the fact that the Coulomb potential energy is converted into kinetic energy implying a greater slowing down time for the recoiling atom. For charge state less than $+6$, the Coulomb interaction is not strong enough to bring the Sm and O atom so close together that they gain enough kinetic energy to destroy the MD cell. With a charge state of $+10$, the MD simulations generate an anomalous great velocity and the MD cell is completely destroyed as the temperature of the cell explodes. The simulation of the loss of many electrons due to Auger cascades for an atom and the change in electron configurations influencing the interatomic potential is hard to achieve especially in the solid state when electron recombinations from neighboring atoms can occur. Therefore careful attention is recommended. The present MD approach (change in the charge state only for the Sm atom) is the only feasible way to include Auger cascades, as the electron clouds and electron rearrangement process cannot be incorporated in the MD program at present.

VI. CONCLUSION

We have studied with the neutrino-induced Doppler-broadening method the slowing down process of a recoiling ^{152}Sm atom in oriented EuO single crystal targets. The crystal-NID measurement permits the selection of a particular potential to reproduce the interaction between Eu-O, Eu-Eu, and O-O. Although the studied potentials do not differ greatly, the fitted lifetime value can select the best interatomic potential. An inherent limitation of this method resides on the knowledge and the precision of the nuclear state lifetime. In the present case the 963.4 keV nuclear state lifetime is measured with sufficient precision by another nuclear method[5] to permit the selection of a potential. The neutrino-induced Doppler technique shows that the Buckingham potential is the most suitable interatomic potential for the interaction between Eu-Eu, Eu-O, and O-O in EuO single crystals at low energies. With this potential, a lifetime of 28.7(1.0) fs is obtained for the 963.4 keV nuclear state in ^{152}Sm, which agrees well with the 29(4) fs given in the literature.

Even at the low recoil energy used [$\sim$3 eV compared to crystal-GRID measurement using $\sim$200 eV (Ref. 30)] it is still possible to see structure on the line shape depending on the orientations. This tells us that the direction of observation plays an important role in the measurement of the GAMS4 spectrometer when single crystals are used. The influence of

Auger cascades which might lead to Coulomb implosion was also studied in the molecular dynamic simulations. Due to the low percentage of Auger emission, it was found to have a minor influence provided the created charge state stays below +6.

ACKNOWLEDGMENTS

This work was supported by the Swiss National Research Fund. The authors are especially grateful to P. Wachter from ETHZ Switzerland and to K. J. Fischer from IFF Forschungszentrum Jülich for making the EuO single crystals available.

[1] E. G. Kessler, G. L. Greene, M. S. Dewey, R. D. Deslattes, H. G. Börner, and F. Hoyler, J. Phys. G **14**, 167 (1988).
[2] J. Jolie, N. Stritt, H. G. Börner, C. Doll, M. Jentschel, S. J. Robinson, and E. G. Kessler, Z. Phys. B **102**, 1 (1997).
[3] A. Kuronen, J. Keinonen, H. G. Börner, and J. Jolie, Phys. Rev. B **52**, 12 640 (1995).
[4] N. Stritt, J. Jolie, M. Jentschel, and H. G. Börner, Phys. Rev. Lett. **78**, 1592 (1997).
[5] A. Jungclaus, T. Belgya, D. P. Diprete, M. Villani, E. L. Johnson, E. M. Baum, C. A. McGrath, S. W. Yates, and N. V. Zamfir, Phys. Rev. C **48**, 1005 (1993).
[6] D. W. Heermann, *Computer Simulation Methods in Theoretical Physics* (Springer Verlag, Berlin, 1986).
[7] P. A. Allen and D. Tildesley, *Computer Simulation of Liquids* (Clarendon, Oxford, 1987).
[8] K. Siegbahn, *Alpha Beta Gamma-Ray Spectroscopy* (North-Holland, Amsterdam, 1965), Vol. 2, p. 1357.
[9] W. Bambynek, B. Graseman, R. W. Fink, H.-U. Freund, H. Mark, C. D. Swift, R. E. Price, and P. V. Rao, Rev. Mod. Phys. **44**, 716 (1972).
[10] M. H. Chem and B. Crasemann, At. Data Nucl. Data Tables **24**, 13 (1979).
[11] I. M. Torrens, *Interatomic Potentials* (Academic, New York, 1972).
[12] R. A. Johnson, J. Phys. F **3**, 295 (1973).
[13] A. A. Abrahamson, Phys. Rev. **178**, 76 (1969).
[14] F. T. Smith, Phys. Rev. A **5**, 1708 (1972).
[15] N. Karasawa and W. Goddard III, J. Chem. Phys. **93**, 7320 (1989).
[16] M. Jentschel, Ph.D. Thesis, Technische Universität Dresden, 1997.
[17] L. Thomas and J. Shanker, Phys. Status Solidi B **181**, 387 (1994).
[18] P. P. Ewald, Ann. Phys. (Leipzig) **64**, 253 (1921).
[19] S. de Leeuw, J. Perram, and E. Smith, Proc. R. Soc. London, Ser. A **373**, 27 (1980).
[20] K. H. Heinig and D. Janssen, ILL Internal Report 92HGB16T, 1992 (unpublished).
[21] S. J. Robinson and J. Jolie, The computer code GRIDDLE; ILL Internal Report RO15T, 1992 (unpublished).
[22] P. Wachter, *Handbook on the Physics and Chemistry of Rare Earths* (North-Holland, Amsterdam, 1977), Chap. 19, p. 507.
[23] T. B. Reed and R. E. Fahey, J. Cryst. Growth **8**, 337 (1971).
[24] E. Kaldis, J. Cryst. Growth **9**, 281 (1971).
[25] K. J. Fischer, U. Köbler, B. Stroka, K. Bickmann, and H. Wenzl, J. Cryst. Growth **128**, 846 (1993).
[26] E. Preuss, B. Krahl-Urban, and R. Butz, *Laue Atlas* (Kernforshungsanlage, Jülich, 1974).
[27] H. G. Börner, J. Jolie, F. Hoyler, S. J. Robinson, M. S. Dewey, G. L. Greene, E. Kessler, and R. D. Deslattes, Phys. Lett. B **215**, 45 (1988).
[28] T. von Egidy *et al.*, Z. Phys. A **286**, 341 (1978).
[29] H. Lehmann (private communication).
[30] M. Jentschel, K. H. Heinig, H. G. Börner, J. Jolie, and E. G. Kessler, Nucl. Instrum. Methods Phys. Res. B **115**, 446 (1996).
[31] J. H. Scofield, Phys. Rev. **179**, 9 (1969).